Recent developments in the modelling of neutron-star crusts

Nicolas Chamel
Université Libre de Bruxelles, Belgium

BLU-ULB
BRUSSELS LABORATORY OF THE UNIVERSE

IAA bruxelles

ULB

fnrs
LA LIBERTÉ DE CHERCHER

HARDY

IReNA-INT workshop, 9-13 December 2024

Outline

1. Neutron superfluid dynamics in neutron-star crusts
   - Small superflow: superfluid density
   - Large superflow: gapless superfluidity
2. Shallow heating in magnetars
   - Possible role of electron captures
3. Conclusions & perspectives

Neutron superfluid dynamics in neutron-star crusts

Spin glitches and superfluidity

$\sim$ 240 pulsars have been found to **suddenly spin up**. Such spin glitches have been also detected in accreting neutron stars.

Review: *Antonopoulou, Haskell, Espinoza, Rep. Prog. Phys. 85, 126901 (2022)*

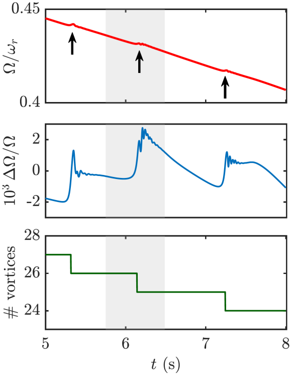

Glitches are thought to be triggered by the **unpinning of quantized vortices**.

Review: *Zhou et al.,Universe 8(12), 641(2022)*

Similar phenomenon observed in ^{4}He and predicted in ultracold atoms.

Poli et al., PRL 131, 223401 (2023)

This suggests the existence of a neutron **superflow in neutron-star crusts**.

How does the neutron superfluid dynamics impact the cooling?

Neutron superfluidity in neutron-star crusts

The **breaking of translational symmetry** leads to the depletion of the superfluid reservoir. *Leggett, PRL 25, 1543 (1970)*

A superflow with velocity $\boldsymbol{V_n}$ induces an average neutron mass current

$$\bar{\boldsymbol{\rho}}_{\boldsymbol{n}} = \rho_{n,s} \boldsymbol{V_n} = \rho_n \frac{m_n}{m_n^\star} \boldsymbol{V_n}.$$

The superfluid density $\rho_{n,s} < \rho_n$ ($m_n^\star > m_n$) is a current-current **response function**.

This "*is not the density of anything*", Richard Feynman.

$\rho_{n,s} \ll \rho_n$ in intermediate crustal layers ($\sim 10^{13}$g cm^{-3})

Chamel, Nucl. Phys. A747, 109 (2005); PRC85, 035801 (2012)

Review: *Chamel, J. Low Temp. Phys. 189, 328 (2017)*

Such depletion has been recently measured in cold atomic condensates in optical traps.
Chauveau et al., PRL 130, 226003 (2023); Tao et al., PRL131,163401 (2023)

Neutron band structure and Fermi surface

In the weak coupling $\Delta/\varepsilon_{\mathrm{F}} \to 0$:

$$\rho_{n,s} \approx \frac{m_n^2}{12\pi^3\hbar^2} \sum_{\alpha} \int_{\mathrm{F}} |\nabla_{\boldsymbol{k}} \varepsilon_{\alpha \boldsymbol{k}}| \mathrm{d}\mathcal{S}^{(\alpha)}$$

Carter et al.,Nucl.Phys.A748,675 (2005)

Similar expression for cold atoms

Pitaevskii et al., PRA71, 053602 (2005)

In intermediate layers:

- cluster size $\sim \lambda_F \ll$ lattice spacing
- periodic potential $\sim 2\varepsilon_F \gg \Delta$

Bragg scattering leads to strong distortions of the Fermi surface.

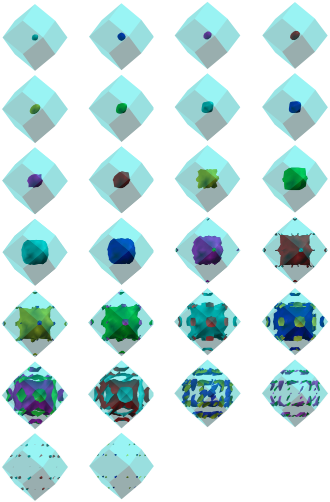

Picture made with XCrySDen

Neglect of pairing?
1D toy models:
Minami&Watanabe,PRR4,033141(2022)
Watanabe&Pethick,PRL119,062701 (2017)

Neutron superfluid fraction and pairing gaps

In the BCS theory, the neutron superfluid density is given by

$$\rho_{n,s} = \frac{m_n^2}{24\pi^3\hbar^2} \sum_{\alpha} \int d^3\boldsymbol{k}\, |\nabla_{\boldsymbol{k}} \varepsilon_{\alpha\boldsymbol{k}}|^2 \frac{|\Delta|^2}{(E_{\alpha\boldsymbol{k}})^3}$$

Carter, Chamel, Haensel, Nucl. Phys. A759, 441 (2005)

Neutron superfluid fraction and pairing gaps

Results of full **3D band-structure calculations with BCS pairing** at baryon density 0.03 fm^{-3} for a body-centered cubic lattice:

Δ (MeV)	Δ/ε_F	$\rho_{n,s}/\rho_{n,f}$
1.59	0.0869	0.0750
1.11	0.0604	0.0750
0.770	0.0420	0.0752
0.535	0.0292	0.0755
0.372	0.0203	0.0760
0.259	0.0141	0.0766
0.180	0.00981	0.0770
0.125	0.00682	0.0774

lattice spacing 47.3 fm

$25 \times 25 \times 25$ grid ($\delta r \sim 0.95$ fm)

$\sim$ 1300 bands (half without pairing)

$\times$ 1360 $\boldsymbol{k} \Rightarrow 10^6$ Bloch states

Chamel, arXiv:2412.05599

$\rho_{n,s} \ll \rho_n$ independently of Δ similarly to fermionic condensate in a 1D periodic optical lattice when potential depth $\gg$ Fermi energy.

Orso& Stringari, Phys. Rev. A109, 023301 (2024)

However, pairing could play a more important role in the nuclear pasta mantle because of weaker periodic potential (potential depth $\lesssim \varepsilon_F$)

Almirante&Urban, Phys.Rev.C109, 045805 (2024); Phys.Rev.C110, 065802(2024)

Sekizawa et al., Phys. Rev.C105, 045807 (2022)

Numerical challenge

The determination of the superfluid fraction is computationally costly because of the high spatial resolution needed: $\delta\ell \lesssim 1$ fm whereas the lattice spacing can reach ~ 110 fm (140 fm for fcc lattice)

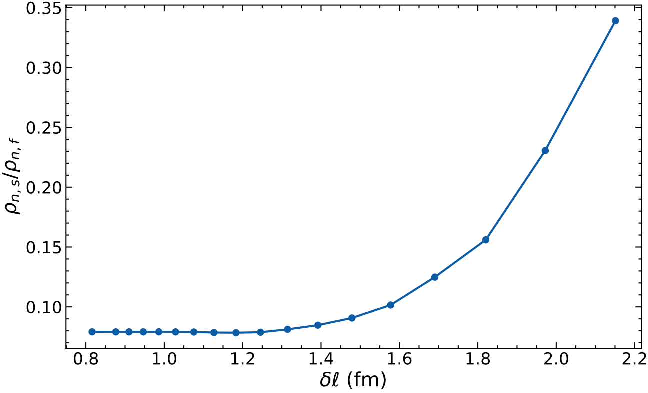

Chamel, arXiv:2412.05599

Superfluid density and cooling

The suppression of the superfluid fraction impacts sound modes:

- transverse lattice phonons are slower,
- longitudinal lattice and superfluid phonons are mixed.

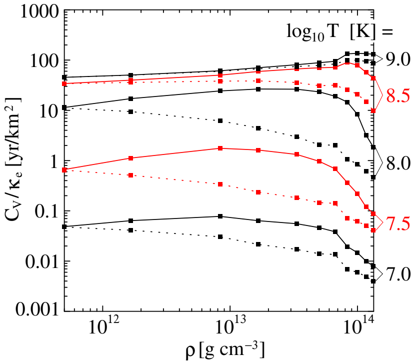

- The specific heat of phonons $\propto (k_B T/\hbar v)^3$ is enhanced.
- Changes in phonon velocities alter electron-phonon scattering therefore the thermal conductivity.

Chamel,Page,Reddy,PRC87,035803(2013)

J.Phys.Conf.Ser.665, 012065(2016)

This may have implications for the cooling of neutron stars.

Finite superflow and Landau's critical velocity

Ignoring spatial inhomogeneities, the flow is frictionless provided $V_n < V_{Ln}$, **Landau's critical velocity**

$$V_{Ln} \equiv V_F \sqrt{\frac{\mu_n}{2\varepsilon_F}\left[\sqrt{1+\left(\frac{\Delta}{\mu_n}\right)^2}-1\right]} \approx \frac{\Delta}{\hbar k_F}$$

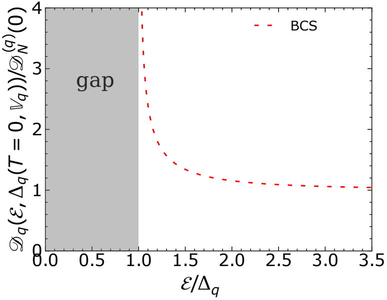

If $V_n < V_{Ln}$, no excitation can be created because of an energy gap: no dissipation.

Allard & Chamel, Phys. Rev. C103, 025804 (2021)

Finite superflow and Landau's critical velocity

Ignoring spatial inhomogeneities, the flow is frictionless provided $V_n < V_{Ln}$, **Landau's critical velocity**

$$V_{Ln} \equiv V_F \sqrt{\frac{\mu_n}{2\varepsilon_F}\left[\sqrt{1+\left(\frac{\Delta}{\mu_n}\right)^2}-1\right]} \approx \frac{\Delta}{\hbar k_F}$$

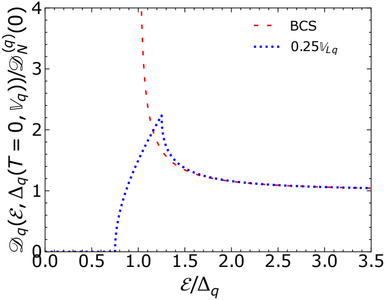

But the gap shrinks with increasing V_n.

Allard & Chamel, Phys. Rev. C103, 025804 (2021)

Finite superflow and Landau's critical velocity

Ignoring spatial inhomogeneities, the flow is frictionless provided $V_n < V_{Ln}$, **Landau's critical velocity**

$$V_{Ln} \equiv V_F \sqrt{\frac{\mu_n}{2\varepsilon_F}\left[\sqrt{1+\left(\frac{\Delta}{\mu_n}\right)^2}-1\right]} \approx \frac{\Delta}{\hbar k_F}$$

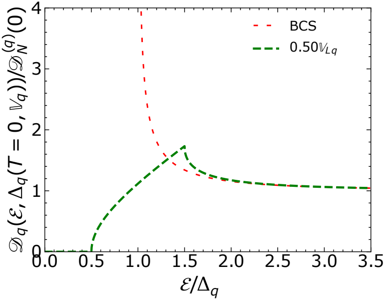

But the gap shrinks with increasing V_n.

Allard & Chamel, Phys. Rev. C103, 025804 (2021)

Finite superflow and Landau's critical velocity

Ignoring spatial inhomogeneities, the flow is frictionless provided $V_n < V_{Ln}$, **Landau's critical velocity**

$$V_{Ln} \equiv V_F \sqrt{\frac{\mu_n}{2\varepsilon_F}\left[\sqrt{1+\left(\frac{\Delta}{\mu_n}\right)^2}-1\right]} \approx \frac{\Delta}{\hbar k_F}$$

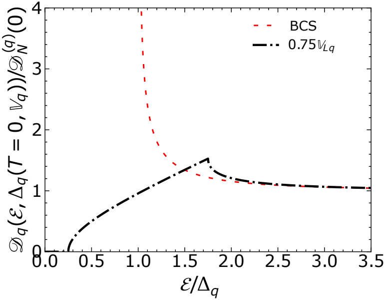

But the gap shrinks with increasing V_n.

Allard & Chamel, Phys. Rev. C103, 025804 (2021)

Finite superflow and Landau's critical velocity

Ignoring spatial inhomogeneities, the flow is frictionless provided $V_n < V_{Ln}$, **Landau's critical velocity**

$$V_{Ln} \equiv V_F \sqrt{\frac{\mu_n}{2\varepsilon_F}\left[\sqrt{1+\left(\frac{\Delta}{\mu_n}\right)^2}-1\right]} \approx \frac{\Delta}{\hbar k_F}$$

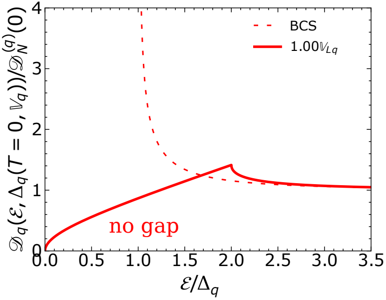

The gap vanishes for $V_n = V_{Ln}$ but superfluidity is not destroyed!

Allard & Chamel, Phys. Rev. C103, 025804 (2021)

Gapless superfluidity

- Δ coincides with the energy gap only for $V_n = 0$
- Δ is the **order parameter** and remains finite for $V_n > V_{Ln}$

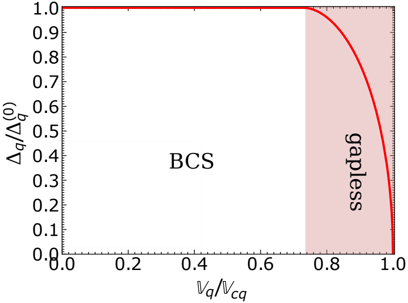

Δ vanishes at the critical velocity

$$V_{cn} \approx \frac{\exp(1)}{2} V_{Ln} \approx 1.4 V_{Ln}$$

The superfluid is gapless for $V_{Ln} \leq V_n < V_{cn}$.

Allard & Chamel, PRC103, 025804 (2021)

A normal fluid of quasiparticles excitations is present even at $T = 0$: the superfluid density is reduced $\rho_{n,s} < \rho_n$ in the gapless phase.

Allard & Chamel, Phys. Rev. C 108, 045801 (2023)

Gapless superfluidity and specific heat

The neutron specific heat is considerably enhanced and comparable to that in the normal phase:

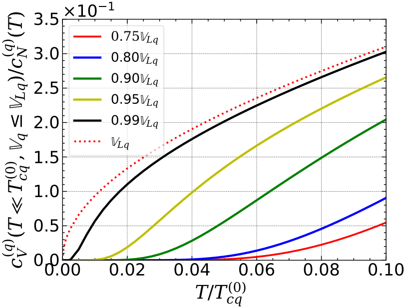

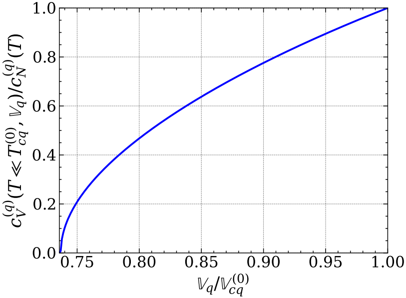

Universal approximate analytical formula have been derived

Allard & Chamel, PRC103, 025804 (2021)

Astrophysical implications

Superfluidity can be probed from the cooling of neutron-star crusts after the end of an accretion episode

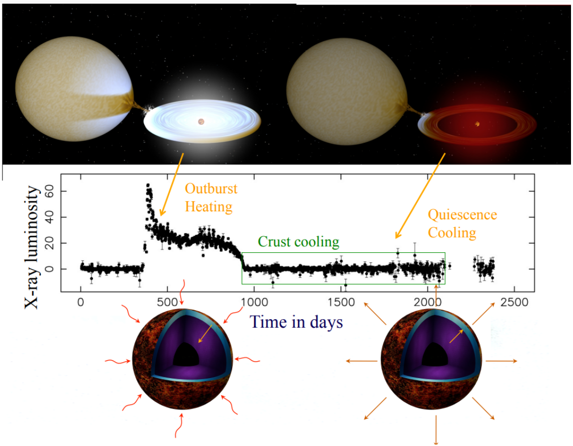

Wijnands, Degenaar, Page, J. Astrophys. Astron. 38, 49, (2017)

Observational puzzles: KS 1731−260

KS 1731−260 appeared **colder than expected** after ∼ 3000 days:

Cackett et al., ApJ 722, L137 (2010)

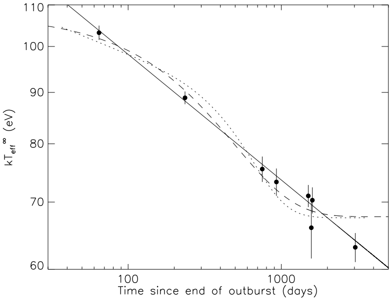

Observational puzzles: KS 1731−260

KS 1731−260 appeared **colder than expected** after ∼ 3000 days:

Cackett et al., ApJ 722, L137 (2010)

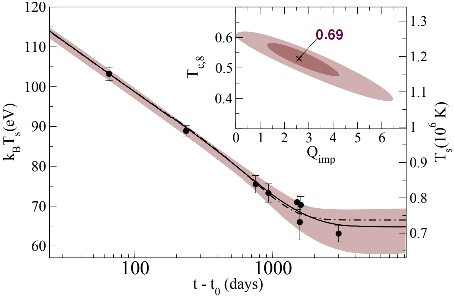

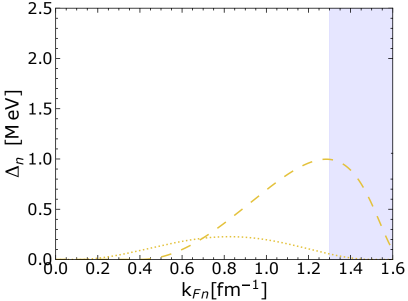

Data could be fitted by **fine tuning the neutron pairing gaps** Δ_n

Turlione et al., A&A 577, A5 (2015)

Observational puzzles: KS 1731−260

KS 1731−260 appeared **colder than expected** after ∼ 3000 days:

Cackett et al., ApJ 722, L137 (2010)

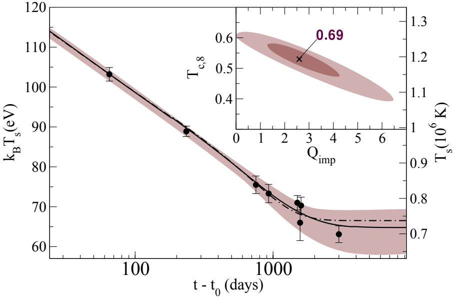

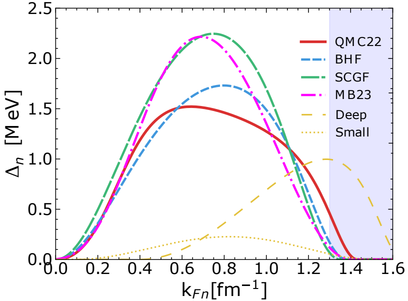

Data could be fitted by **fine tuning the neutron pairing gaps** Δ_n

Turlione et al., A&A 577, A5 (2015)

But these empirical gaps are not compatible with latest microscopic calculations based on different many-body approaches.

Observational puzzles: KS 1731−260

KS 1731−260 appeared **colder than expected** after ∼ 3000 days:

Cackett et al., ApJ 722, L137 (2010)

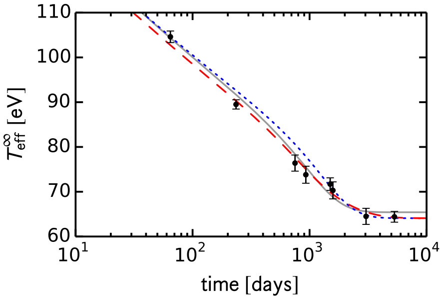

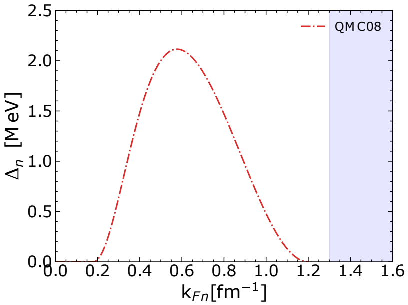

Data could be fitted by **considering the vanishing of neutron pairing gaps** in the densest crustal layers, as predicted by quantum Monte Carlo calculations

Deibel et al., ApJ 839, 95 (2017)

Observational puzzles: KS 1731−260

KS 1731−260 appeared **colder than expected** after ∼ 3000 days:

Cackett et al., ApJ 722, L137 (2010)

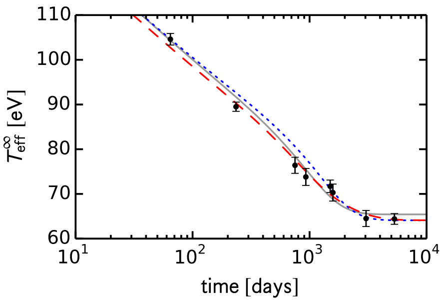

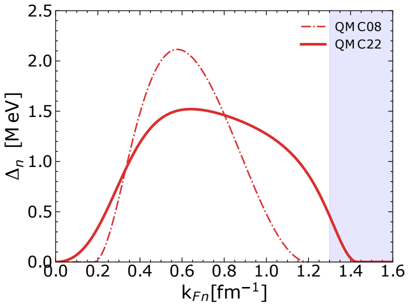

But this conclusion is no longer supported by more recent quantum Monte Carlo calculations (in agreement with other microscopic approaches).

Observational puzzles: MXB 1659−29

MXB 1659−29 exhibited an **unexpected late-time cooling**:

Cackett et al., ApJ 774, 131 (2013)

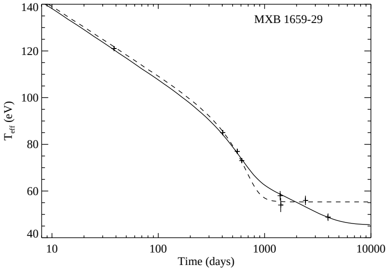

Observational puzzles: MXB 1659−29

MXB 1659−29 exhibited an **unexpected late-time cooling**:

Cackett et al., ApJ 774, 131 (2013)

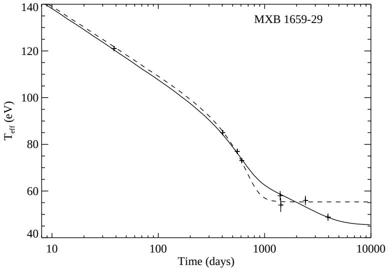

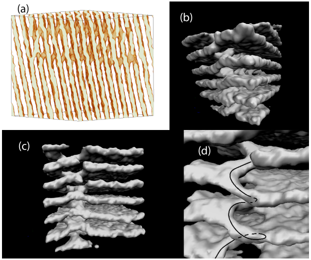

Data could be fitted by considering **disordered nuclear pasta** in the densest crustal layers, as predicted by classical molecular dynamics (at $\bar{n} = 0.05$ fm^{-3}, $T \approx 1$ MeV and $Y_p \approx 0.4$).

Horowitz et al., PRL 114, 031102 (2015)

Observational puzzles: MXB 1659−29

MXB 1659−29 exhibited an **unexpected late-time cooling**:

Cackett et al., ApJ 774, 131 (2013)

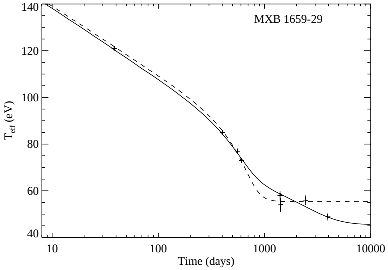

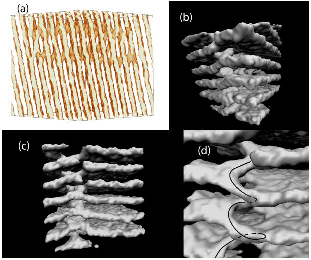

Data could be fitted by considering **disordered nuclear pasta** in the densest crustal layers, as predicted by classical molecular dynamics (at $\bar{n} = 0.05$ fm^{-3}, $T \approx 1$ MeV and $Y_p \approx 0.4$).

Horowitz et al., PRL 114, 031102 (2015)

But this conclusion was not confirmed by subsequent simulations.

Nandi & Schramm, ApJ 852, 135 (2018)

Classical vs quantum recipe of nuclear pasta

Extended Thomas Fermi (ETF) calculations with/out shell effects (SI):

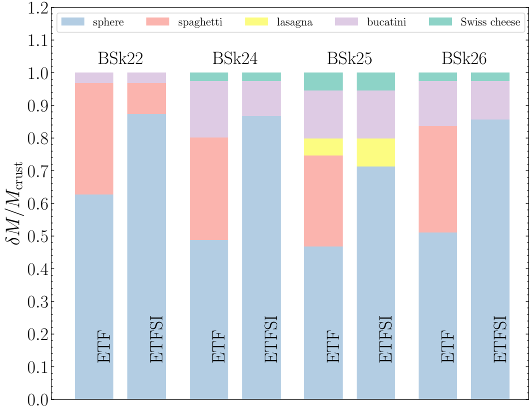

The region containing pasta shrinks dramatically with shell effects!

Shchechilin, Chamel, Pearson, PRC108, 025805 (2023); PRC109, 055802 (2024)

Neutron diffusion in accreted crusts

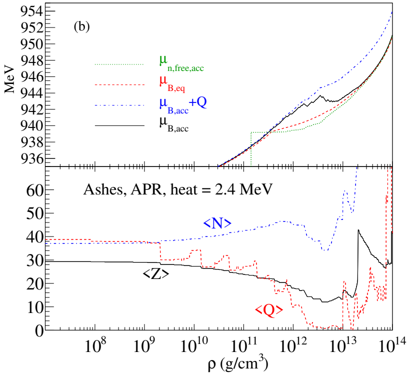

In traditional accreted crust models, neutrons are emitted all at once by nuclei and sink with them.

This leads to **spurious jump of the neutron chemical potential**

Steiner, PRC85, 055804 (2012)

Free neutrons actually appear at lower density and pressure

Chamel et al., PRC91, 055803 (2015)

Thermodynamically consistent treatment by Gusakov & Chugunov:

- same equation of state as catalyzed crust despite composition
- considerably **reduced heating** $\sim$ 0.3 vs $\sim$ 1.5 MeV/nucleon

Gusakov&Chugunov, PRL 124, 191101 (2020); PRD104, L081301 (2021)

Cooling of KS 1731−260 revisited

We have run cooling simulations using `crustcool` code modified to account for **neutron diffusion with realistic pairing gaps**:

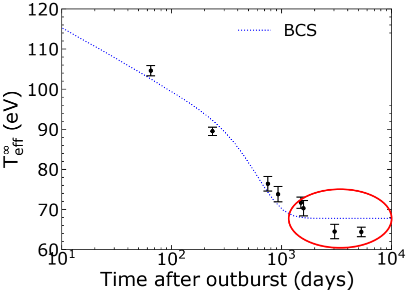

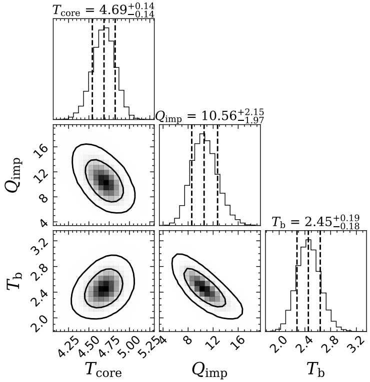

In the absence of superflow (BCS), the thermal relaxation is still too fast due to the suppression of the neutron specific heat.

Cooling of KS 1731−260 revisited

We have run cooling simulations using `crustcool` code modified to account for **neutron diffusion with realistic pairing gaps**:

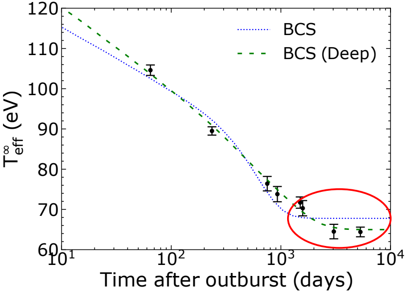

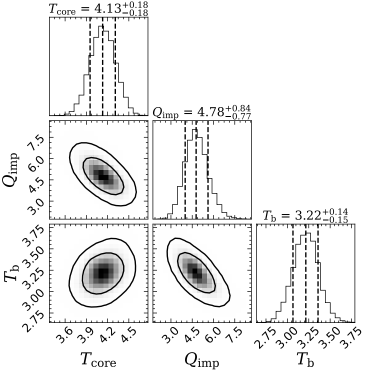

Observations can only be fitted by using unrealistic pairing gaps.

Cooling of KS 1731−260 revisited

We have run new cooling simulations accounting for **neutron diffusion and gapless superfluidity with realistic pairing gaps**:

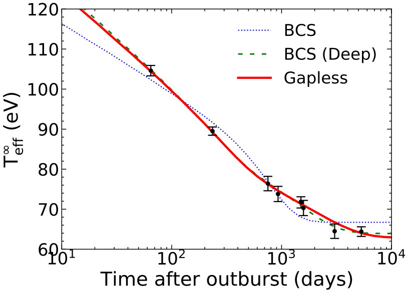

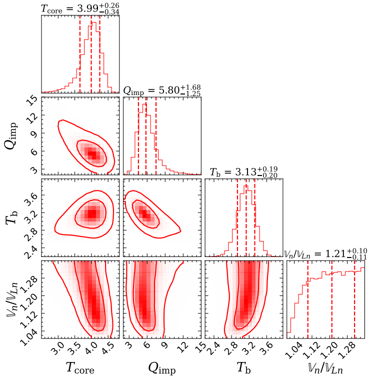

Gapless superfluidity can naturally explain observations.

Allard & Chamel, PRL 132, 181001 (2024)

Cooling of MXB 1659−29 revisited

We have run new cooling simulations accounting for **neutron diffusion and gapless superfluidity with realistic pairing gaps**:

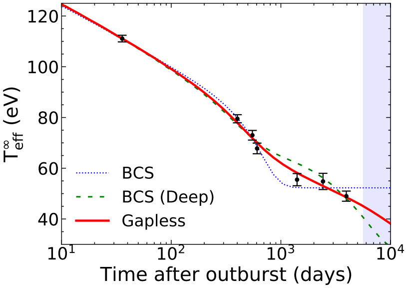

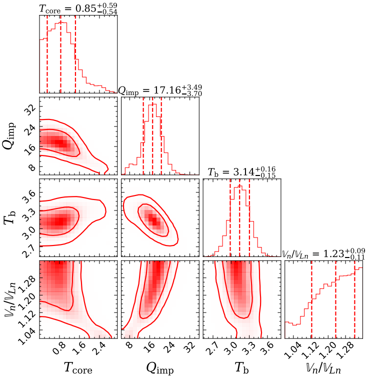

Gapless superfluidity yields again the best fits to data.

Allard & Chamel, PRL 132, 181001 (2024)

Gapless superfluidity and delayed cooling

- In both Haensel&Zdunik and Gusakov&Chugunov models, the neutron specific heat is negligible irrespective of neutron diffusion
- Cooling is dictated by electrons and ions

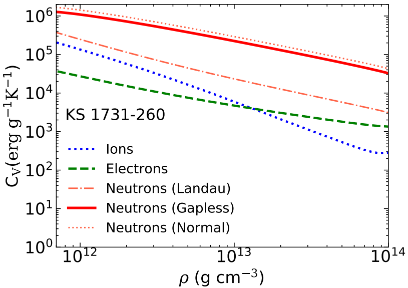

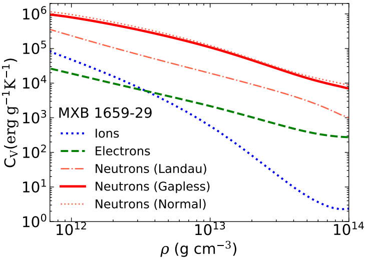

Whereas in the gapless phase, the neutron specific heat dominates thus leading to a delayed cooling.

Cooling of MXB 1659−29 after second outburst

We have run new cooling simulations for the second outburst keeping fixed the core temperature:

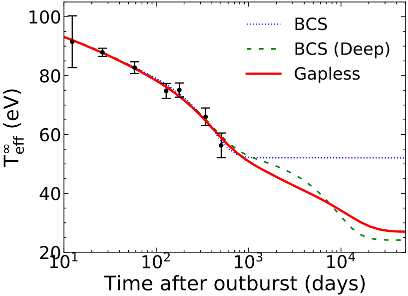

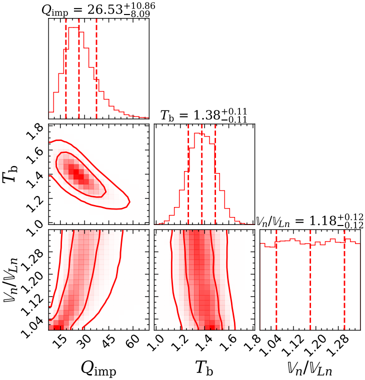

Allowing for gapless superfluidity leads to very different predictions.

Allard & Chamel, PRL 132, 181001 (2024)

Spectral fits of MXB 1659−29

Cackett et al. (2013) actually presented 4 different spectral fits for the last observation after the end of the first outburst:

model	$k_B T_{eff}^{\infty}$ (eV)	N_H (cm^{-2})
absorbed atmosphere	**49.0±2.0**	**2×10^{21} (observations)**
atm.+power law $\Gamma = 1.5$	45.0±3.0	2×10^{21} (observations)
atm.+power law $\Gamma = 2$	43.0±5.0	2×10^{21} (observations)
absorbed atmosphere	55±3.0	$(4.7 \pm 1.3) \times 10^{21}$ (free)

In recent studies, the last fit (the only one consistent with standard cooling) has been adopted. Why discarding other fits?

- Large variations of N_H possibly due to disk precession.
- But fitting N_H through both outbursts did not show variations.

Parikh et al., A&A 624, A84 (2019)

Gapless superfluidity can explain all spectral fits

Allard&Chamel, Eur. Phys. J. A60, 116 (2024)

Sensitivity analyses

Varying the envelope composition, neutron-star mass and radius, accretion rate, gapless superfluidity still yields the best fits:

After end of the first outburst of MXB 1659−29:

With gapless superfluidity

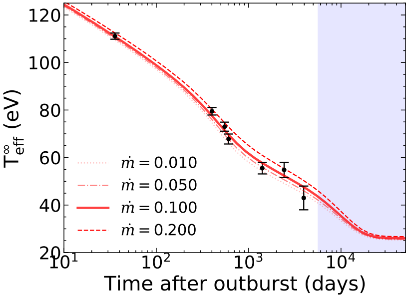

With BCS superfluidity

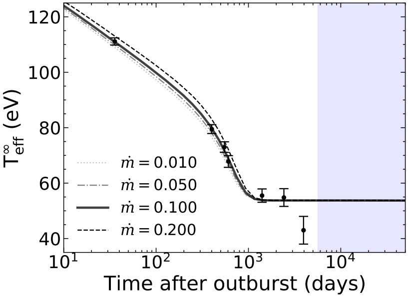

Similar conclusions for KS 1731−260.

Allard&Chamel, Eur. Phys. J. A60, 116 (2024)

Different cooling scenarios

Different models lead to different predictions for the long-term cooling:

Since the end of the second outburst of MXB 1659−29:

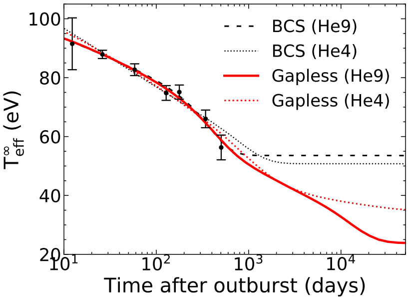

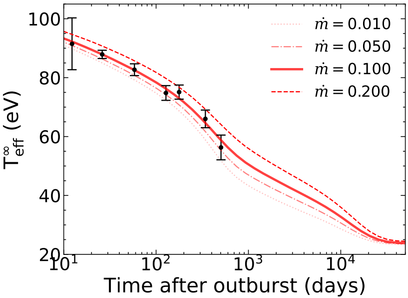

Allard&Chamel, Eur. Phys. J. A60, 116 (2024)

Further observations are crucially needed!

Stability of the super Landau superflow?

Fully self-consistent time-dependent quantum simulations of the **motion of a single cluster through the neutron superfluid**:

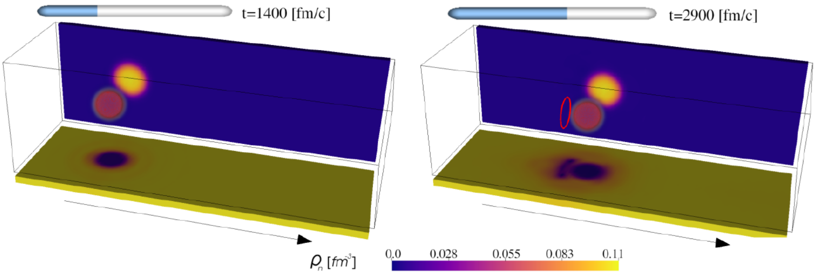

The gapless superfluid is stable in deep crust but in shallow layers Cooper pair breaking leads to the **formation of vortex rings**: onset of quantum turbulence? Glitch triggering mechanism?

Peçak, Chamel, Zdanowicz et al., Phys. Rev. X 14, 041054 (2024)

Conclusions I

The breaking of translation symmetry in the crust of neutron stars leads to the depletion of the neutron superfluid reservoir.

- The neutron superfluid fraction is suppressed due to **Bragg scattering** independently of BCS pairing
- This suppression alters thermal properties and potentially the cooling of neutron stars.
- But beyond BCS calculations are needed to draw more definite conclusions.

Vortex pinning induces a neutron superflow in the crust.

- When $V_n > V_{Ln}$, superfluidity becomes **gapless**.
- Gapless superfluidity naturally explains the observed cooling of transiently accreting neutron stars due to the huge specific heat.
- This scenario could be tested with further observations.

Shallow heating in magnetars

Highly-magnetized neutron stars

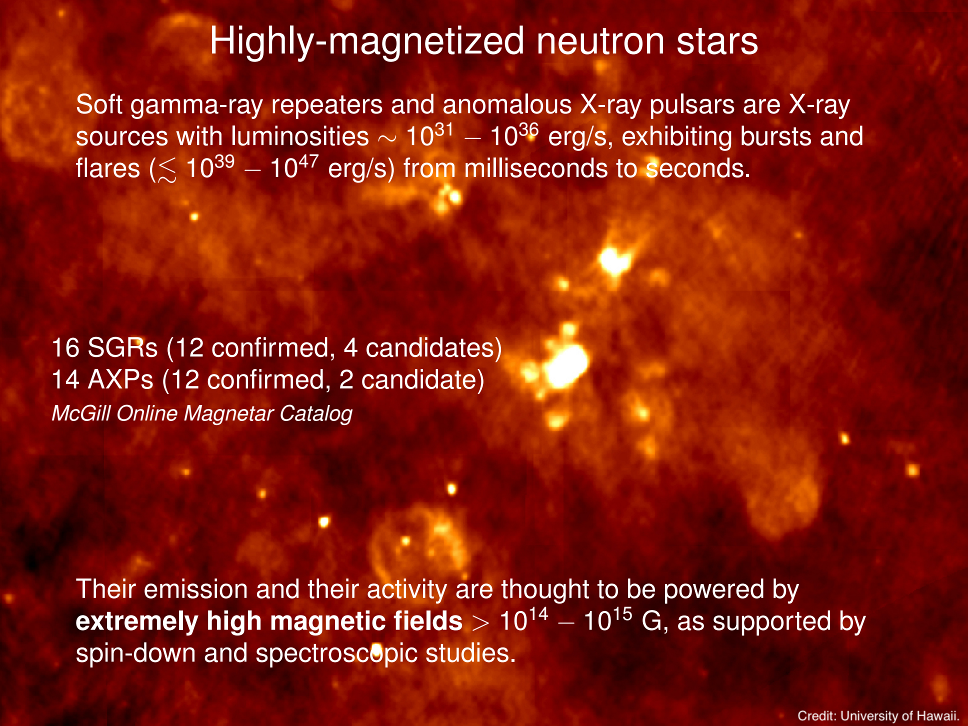

Soft gamma-ray repeaters and anomalous X-ray pulsars are X-ray sources with luminosities $\sim 10^{31} - 10^{36}$ erg/s, exhibiting bursts and flares ($\lesssim 10^{39} - 10^{47}$ erg/s) from milliseconds to seconds.

16 SGRs (12 confirmed, 4 candidates)
14 AXPs (12 confirmed, 2 candidate)
McGill Online Magnetar Catalog

Their emission and their activity are thought to be powered by **extremely high magnetic fields** $> 10^{14} - 10^{15}$ G, as supported by spin-down and spectroscopic studies.

Credit: University of Hawaii.

Magnetar outbursts

Enhancements of the persistent X-ray flux by several orders of magnitude lasting for weeks or even years have been also observed:

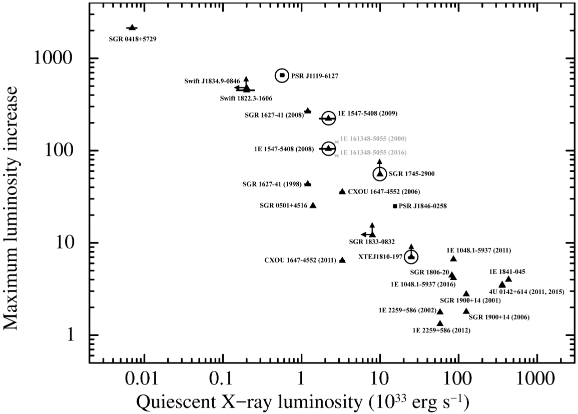

Coti Zelati et al., MNRAS 474, 961 (2018)

Outbursts are usually attributed to some **internal heating**.

Internal heating source

A popular explanation involves the dissipation of mechanical energy during crust quakes.

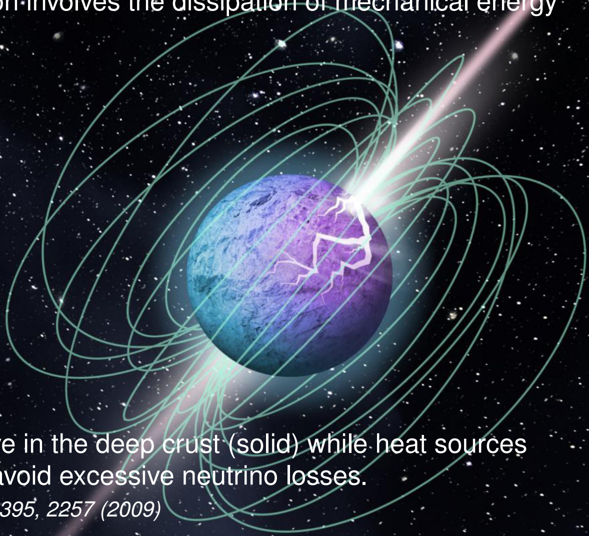

Caveat: only effective in the deep crust (solid) while heat sources must be shallow to avoid excessive neutrino losses.

Kaminker et al., MNRAS 395, 2257 (2009)

Critical review of various scenarios:

Beloborodov & Li, ApJ 833, 261 (2016)

McGill University Graphic Design Team

Heating from electron captures

The compression of matter accompanying the **decay of the magnetic field** may induce **electron captures in the crust**. This is analogous to accreting neutron stars.

Cooper & Kaplan, ApJ 708, L80 (2010)

Two-step process:

- first electron capture in quasi equilibrium (B decay time scale)
$$(A,Z) + e^- \rightarrow (A,Z-1) + \nu_e$$
- second electron capture off equilibrium **releasing some heat** $\mathcal{Q}$
$$(A,Z-1) + e^- \rightarrow (A,Z-2) + \nu_e + \mathcal{Q}$$

Further compression may give rise to **delayed neutron emission**
$$(A,Z) + e^- \rightarrow (A-\Delta N, Z-1) + \Delta N\, n + \nu_e$$

Cooper&Kaplan assumed same heat sources as in accreting neutron stars. However, physical conditions are completely different.

Chamel,Fantina,Suleiman,Zdunik,Haensel, Universe 7(6), 193 (2021)

Consequence of a high internal magnetic field

In the outer crust, **electrons are free and relativistic.** Their motion perpendicular to ***B*** is quantized into **Rabi levels**:

$$e_\nu = \sqrt{c^2 p_z^2 + m_e^2 c^4 (1 + 2\nu B_\star)}$$

where $\nu = 0, 1, 2...$ and $\mathbf{B}_\star = \mathbf{B}/\mathbf{B_c}$

with $\mathbf{B_{rel}} = \dfrac{\mathbf{m_e^2 c^3}}{\hbar \mathbf{e}} \simeq \mathbf{4.4} \times \mathbf{10^{13}}$ G.

Rabi, Z.Phys.49, 507 (1928)

The equation of state is **very stiff**

$$\rho \approx \rho_s \left(1 + \sqrt{\frac{P}{P_0}}\right) , \quad P_0 \simeq 1.45 \times 10^{20} (B/10^{12}\ \mathrm{G})^{7/5} \left(\frac{Z}{A}\right)^2 \mathrm{dyn\,cm}^{-2}$$

Chamel et al., PRC86, 055804 (2012); Mutafchieva et al., PRC 99, 055805 (2019)

The composition of the crust can be also altered because magnetars are born with very strong **B** that can be sustained for $> 10^3$ yrs.
Duncan&Thompson, ApJ392,L9(1992)

Analytical determination of the crust composition

Usual approach: numerical minimization of the Gibbs free energy per nucleon at different pressures P (assuming full equilibrium)

Lai& Shapiro, ApJ 383, 745 (1991)

- layers can be easily missed if δP not small enough
- numerically costly (calculations for a range of B)

New approach: iterative minimization of the pressures between adjacent crustal layers (approximate analytical formulas)

Chamel, PRC 101, 032801(R) (2020)

Chamel&Stoyanov,PRC 101, 065802 (2020)

- very accurate ($\delta P/P \sim 0.1\%$)
- nuclear abundances and depths at no additional cost
- $\sim 10^4 - 10^6$ times faster depending on B

Freely available computer codes for very low- and very high B:

`http://doi.org/10.5281/zenodo.3839787`

Onset of electron captures with magnetic fields

Threshold density and pressure of electron captures by ^{56}Fe:

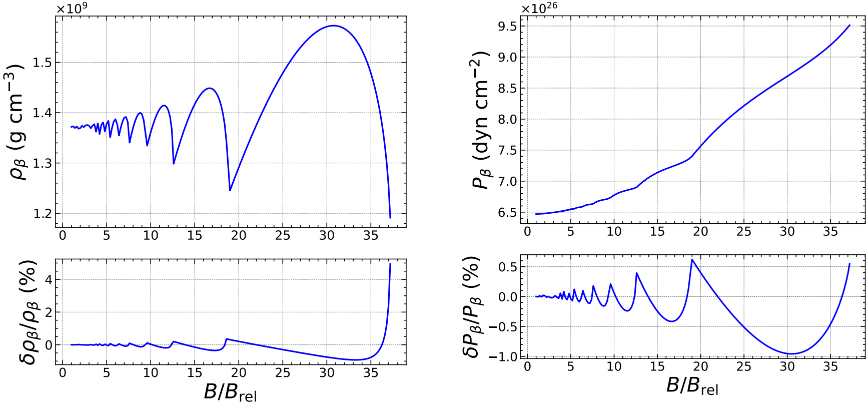

Onset of electron captures with magnetic fields

Threshold density and pressure of electron captures by ^{56}Fe:

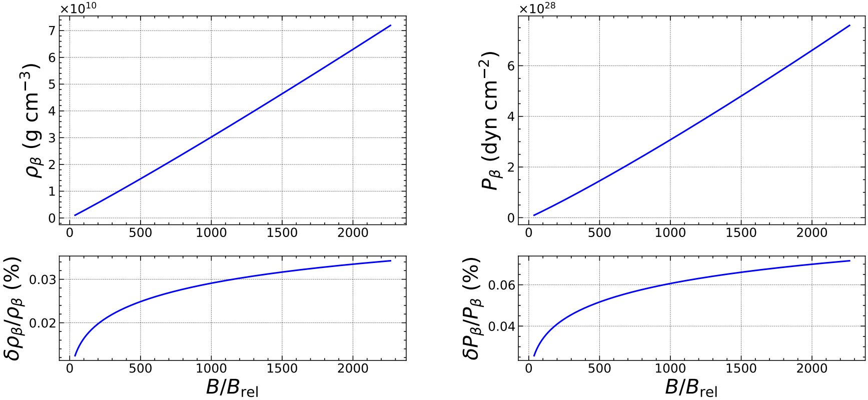

We have obtained very **accurate analytical expressions for any nucleus and arbitrary magnetic fields.**

Chamel&Fantina, Universe 8(6), 328 (2022)

Heat released by electron captures

Maximum possible heat released by electron capture by ^{56}Fe:

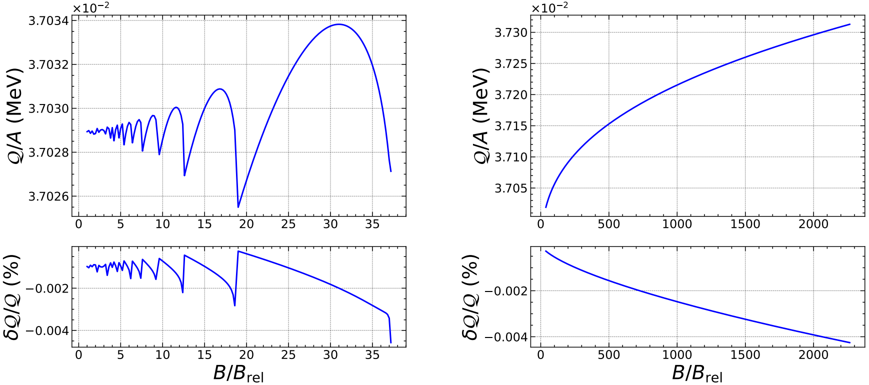

Chamel&Fantina, Universe 8(6), 328 (2022)

$\mathcal{Q}$ is essentially **independent of B** and is determined by nuclear masses and excitations energies.

Full data for ρ_β, P_β, $\mathcal{Q}$ for other nuclei can be downloaded here:

`https://zenodo.org/records/6604639`

Magnetars vs accreting neutron stars

- Same electron captures in all magnetars vs burst-dependent in accreting neutron stars
- Most of the heat is released at densities and pressures **substantially higher than in accreting neutron stars.**
- Heat sources are not uniformly distributed but are **concentrated** at densities $\rho \sim 10^{10} - 10^{11}$ g cm^{-3} ($P \sim 10^{29} - 10^{30}$ dyn cm^{-2}).

In both cases:

- The maximum heat is essentially **independent of *B* and of the crust structure** (assumption of solid crust not required).
- The heat is **mainly determined by the Q values in vacuum**

$$\mathcal{Q}(A,Z) \approx Q_{\rm EC}(A,Z-1) - Q_{\rm EC}(A,Z)$$

$$Q_{\rm EC}(A,Z) = M'(A,Z)c^2 - M'(A,Z-1)c^2$$

- Additional heat may be deposited by **pycnonuclear fusions.**

Conclusions II

Electron captures induced by magnetic field decay in the outer crust of magnetars may potentially be a viable internal heating source.

- This mechanism operates **whether the crust is solid or not**, and independently of its structure.
- The time scales are **comparable to SGR/AXP kinematic ages**.
- Locations at densities $10^{10} - 10^{11}$ g cm^{-3} (for $B \sim 10^{16} - 10^{17}$ G) and power $W^{\infty} \sim 10^{35} - 10^{36}$ erg/s **consistent with cooling**.

Chamel et al., Universe 7(6), 193 (2021)

Simulations of the full magnetothermal evolutions (combined with reaction networks) are required to confirm this scenario.

- Very fast code to compute the initial crustal composition: `http://doi.org/10.5281/zenodo.3839787`
- Very accurate analytical formulas for ρ_β, P_β, $\mathcal{Q}$ for any **B**: *Chamel&Fantina, Universe 8(6), 328 (2022)*
- Numerical data set: `https://zenodo.org/records/6604639`